CO₂ Flushing Triggers Paroxysmal Eruptions at Open Conduit Basaltic Volcanoes

Luca Caricchi[1] , **Chiara P. Montagna[2]** , **Alessandro Aiuppa[3]** , **Joao Lages[3,4]** , **Giancarlo Tamburello[5]**, and **Paolo Papale[2]**

[1]Department of Earth Sciences, University of Geneva, Geneva, Switzerland, [2]Istituto Nazionale di Geofisica e Vulcanologia, Pisa, Italy, [3]Dipartimento di Scienze della Terra e del Mare, Università di Palermo, Palermo, Italy, [4]Now at Earth Sciences Department, University College London, London, UK, [5]Istituto Nazionale di Geofisica e Vulcanologia, Bologna, Italy

Abstract Open conduit volcanoes erupt with the highest frequency on Earth. Their activity is characterized by an outgassing flux that largely exceeds the gas that could be released by the erupted magma; and by frequent small explosions intercalated by larger events that pose a significant risk to locals, tourists, and scientists. Thus, identifying the signs of an impending larger explosion is of utmost importance for the mitigation of volcanic hazard. Larger explosive events have been associated with the sudden ascent of volatile rich magmas, however, where and why magma accumulates within the plumbing system remains unclear. Here we show that the interaction between CO_2-rich fluids and magma spontaneously leads to the accumulation of volatile-rich, low density and gravitationally unstable magma at depth, without the requirement of permeability barriers. CO_2-flushing forces the exsolution of water and the increase of magma viscosity, which proceeds from the bottom of the magma column upward. This rheological configuration unavoidably leads to the progressive thickening of a gas-rich and low density (i.e., gravitationally unstable) layer at the bottom of the feeding system. Our calculations account for observations, gas monitoring and petrological data; moreover, they provide a basis to trace the approach to deeply triggered large or paroxysmal eruptions and estimate their size from monitoring data. Our model is finally applied to Stromboli volcano, an emblematic example of open conduit volcano, but can be applied to any other open conduit volcano globally and offers a framework to anticipate the occurrence of unexpectedly large eruptions.

Plain Language Summary Open conduit volcanoes erupt with the highest frequency on Earth and release significantly more gas than magma. Their activity is characterized by almost continuous and small explosions that are intercalated by significantly larger explosive events. The relatively continuous explosive activity makes these volcanoes attractive both for scientific research and tourism, however, unexpectedly large explosions pose a significant risk to scientists and tourists. The excess gas these volcanoes release is CO_2-rich and its interaction with magma leads to the accumulation of gas-rich and low-density magma at depth, below higher density magma. We suggest that the gravitational destabilization of this deep and gas rich magma is ultimately responsible for the large explosions that punctuate the activity of open conduit volcanoes. The approach to this larger events can be traced with continuous gas monitoring, which therefore provides a unique opportunity to anticipate this otherwise unexpected explosions.

1. Introduction

Paroxysmal explosions are sudden and violent blasts that occasionally interrupt the mild explosive activity of persistently active, mafic open-vent volcanoes worldwide, such as Stromboli (Andronico et al., 2021; Edmonds et al., 2022; Papale, 2018; Rosi et al., 2000; Vergniolle & Métrich, 2022) and Etna (Corsaro & Miraglia, 2022) in Italy; Villarrica in Chile (Aiuppa et al., 2017). Forecasting these events, and understanding their driving mechanisms, have traditionally been hindered by the apparent lack of precursory changes in surface activity, which point to a deep trigger (Aiuppa et al., 2010; Allard, 2010; Harris & Ripepe, 2007). However, continuous instrumental gas observations reveal that these apparently unexpected eruptions are in fact preceded by weeks/months of progressive escalation of carbon dioxide (CO_2) emissions from the crater plume (Aiuppa et al., 2010, 2017), indicating deeply sourced (CO_2-rich) gas is implicated as an eruption trigger. Additionally, the analysis of the frequency of small explosions (hourly explosion frequency, HEF), shows an increase contemporaneous with the increase of carbon dioxide emission in the period preceding large or paroxysmal eruptions (Andronico

et al., 2021), even if such increase of frequency does not always culminate into a large explosion (Laiolo et al., 2022). Petrology and diffusion chronometry confirm that the period of the enhanced CO_2 emissions and increased HEF is accompanied by input of hotter magma to the shallowest portion of the plumbing system.

Existing models for the trigger mechanism of large eruptions and paroxysms provide abundant evidence that implicate the arrival of deep and CO_2-rich magma from depth (Aiuppa et al., 2009, 2010, 2021; Edmonds et al., 2022; Métrich, 2005; Métrich et al., 2021; Petrone et al., 2022). Here, we focus on determining the mechanism that triggers such sudden rise of gas-rich magma from depth. If the process ultimately leading to the ascent of this gas-rich magma from depth operated rapidly and randomly, these events would be impossible to anticipate. However, recent gas monitoring data for Stromboli volcano (Italy) suggest that before large explosions, there is a prolonged period of variability in gas fluxes and chemistry that may provide a means to anticipate the occurrence and magnitude of these events (Aiuppa et al., 2021).

We use numerical and petrological modeling to assess what are the potential causes for the rapid ascent of gas rich magma from depth, which is ultimately responsible for large eruptions at open conduit volcanoes. We first introduce the model that was inspired by the measurements collected at Stromboli volcano and present its results. We finally apply the model to the major explosion of the 19th of July 2020 because it is one of the strongest of the last 20 years of instrumental record (Andronico et al., 2021), we have data providing a continuous record of CO_2, H_2O, and SO_2 emissions and the petrological characterization of the eruption has been completed (Voloschina et al., 2023).

2. Observation-Driven Model Design

Data and observations gathered on the activity of Stromboli and other open conduit volcanoes show that the amount of released magmatic volatiles is significantly larger than the mass of erupted magma (Aiuppa et al., 2010; Allard, 2010; Burton et al., 2007; Edmonds et al., 2022; Métrich et al., 2010; Shinohara, 2008). This is incontrovertible evidence that excess fluids are present within volcanic plumbing systems, and they can separate and percolate through the magmatic systems (flushing; Aiuppa et al., 2010, 2021; Allard, 2010; Blundy et al., 2010; Girona et al., 2015; Yoshimura & Nakamura, 2011). This leads to chemical disequilibrium between magmas stored in different portions of the plumbing system and the migrating fluids. The re-equilibration between percolating fluids and the resident magma impacts the chemistry of both fluids and magma, and the chemistry of the gases released at the surface of active volcanic systems (Blundy et al., 2010; Caricchi et al., 2018; Yoshimura & Nakamura, 2010, 2011). Thus, excess fluids-magma interaction must be considered when attempting to interpret variations of monitoring signals.

Continuous gas monitoring data collected at Stromboli volcano for CO_2 and SO_2 emissions from June 2018 to January 2021 (Aiuppa et al., 2021) and the data presented here for CO_2 and H_2O measured in 2020 (Figure 1), show a progressive increase of CO_2 in the phase leading to major explosions. These data suggest that the paroxysmal and major eruptions that occurred during this period were triggered by a process that is protracted in time as also suggested by diffusion chronometry (Métrich et al., 2021; Petrone et al., 2022).

3. Flushing Model

Because of the large excess of emitted gases with respect to the erupted magma (e.g., Edmonds et al., 2022), we model the interaction between an excess volatile phase and mafic magma distributed over a range of depths within a plumbing system. Excess fluids released at depth are CO_2-rich (e.g., Newman & Lowenstern, 2002) and therefore we simulate the chemical interaction between CO_2-rich fluids released at the base of a crustal plumbing system and magma distributed over several kilometers depth using SOLWCAD (Papale et al., 2006), which computes the equilibrium saturation conditions for a mixture of water and CO_2 volatile phase and a silicate melt of generic composition (Papale et al., 2022).

At the end of this contribution we apply our model to Stromboli volcano, thus we consider that the plumbing system is filled with a magma with the composition of one of the most mafic melt inclusions measured by Métrich et al. (2010; Sample ST531, M.I. 4b). While the exact chemistry of melt can affect H_2O and CO_2 solubility (Iacovino et al., 2021), we focus on one composition to trace the impact of progressive addition of an excess fluid phase on the chemistry of the gas released at the top of the column and dissolved in the magma at different depths.
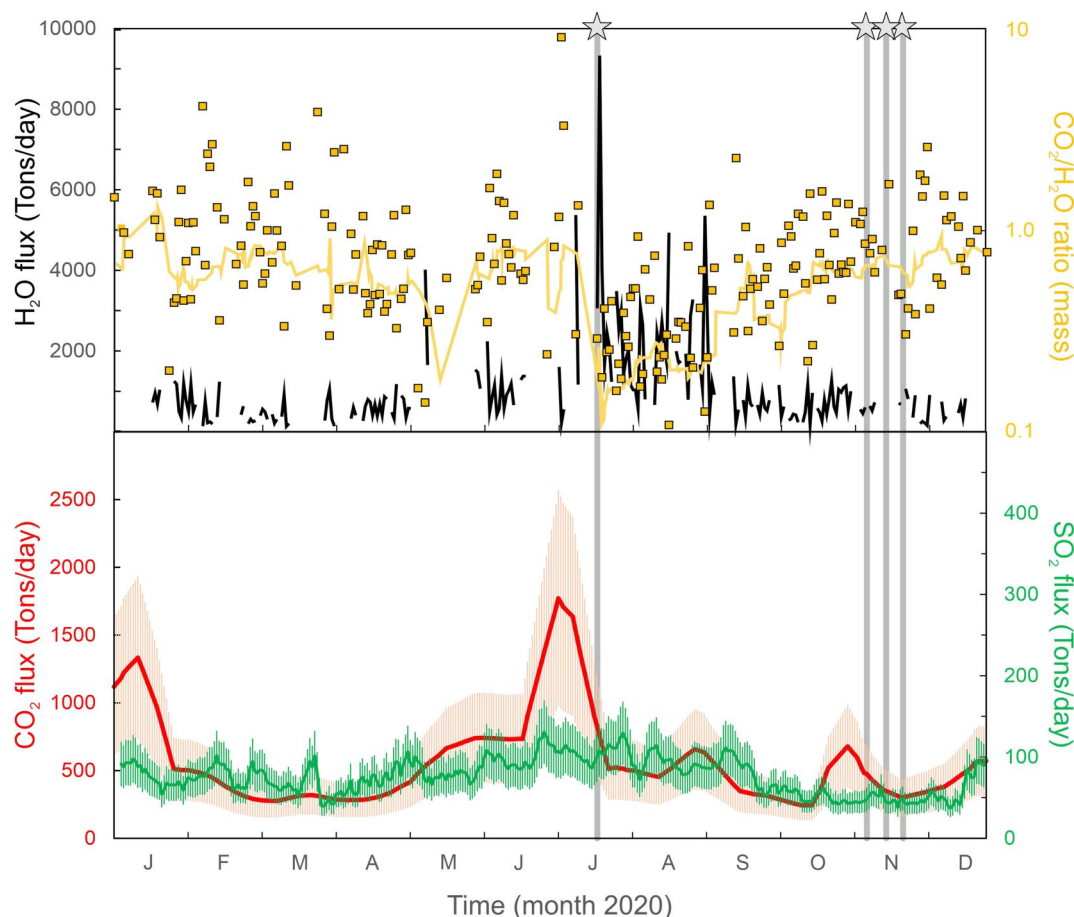
Figure 1. Volcanic gas plume time-series from Stromboli volcano. (a) CO_2/H_2O mass ratios in the plume (squares; the orange solid line is a 2-week mobile average) during the year 2020. Results are obtained by processing (with the methodology detailed in Aiuppa et al. (2010)) plume concentration time-series acquired by a permanent Multi-GAS network installed on Stromboli's summit. The plume H_2O flux (black line) is derived by combining SO_2 fluxes (green line, bottom panel) and measured H_2O/SO_2 ratios in the plume (from Multi-GAS). The SO_2 fluxes (data reported in Aiuppa et al. (2021)) are derived from processing of images acquired by a permanent UV Camera system (Delle Donne et al., 2022); (b) daily averaged CO_2 (red) and SO_2 (green) fluxes, in t/d. The CO_2 flux (data from Aiuppa et al. (2021)) is obtained by combining the UV-Camera based SO_2 fluxes with the Multi-GAS derived CO_2/SO_2 ratios. The bars indicate errors at 1 standard deviation (±45% and ±30% for CO_2 and SO_2, respectively). The vertical gray bars with stars mark timing of larger than ordinary (major) explosions (Andronico et al., 2021) on July 19 and November 10, 16, and 21.

We consider that an excess fluid phase ($xCO_2 = 0.94$) is injected at the base of a magma column and rises distributed in bubbles with Stokes velocity controlled by their radius, the viscosity of the melt and the density contrast between melt and excess fluid phase. We divide the column in steps of length equivalent to a pressure drop in the magma column of 10 MPa (300 m for an average magma column density of $\rho = 3,000 \, \text{kg/m}^3$). At each consecutive step, the excess fluid phase equilibrates with the melt, which induces a change of H_2O and CO_2 fraction in both melt and excess fluid phases until the magma column is fully equilibrated with the excess fluid injected at the base of the column (Figure 2). This assumption is valid only if the bubbles move through one step of the column over timescales that are longer than the chemical fluid-magma re-equilibration timescale. To test under which conditions this last assumption is verified we calculate the ratio between the volatile diffusion timescales and the Stokes rise time, calculated as the step length divided by Stokes velocity (Figure 3). As CO_2 has an order of magnitude lower diffusivity than H_2O (Watson, 1991), timescales are an order of magnitude larger, and we consider only the diffusivity of CO_2 $D = 10^{-10} \, \text{m}^2/\text{s}$ (Yoshimura & Nakamura, 2011). Our calculations show that for a range of melt viscosities (from 1 to 1,000 Pa s; Vona et al., 2011) appropriate for mafic magmas such as those erupted at Stromboli, and bubbles of radius smaller than about 1 mm, the timescales of diffusive re-equilibration are always shorter than the Stokes timescale, and therefore for relatively small bubbles
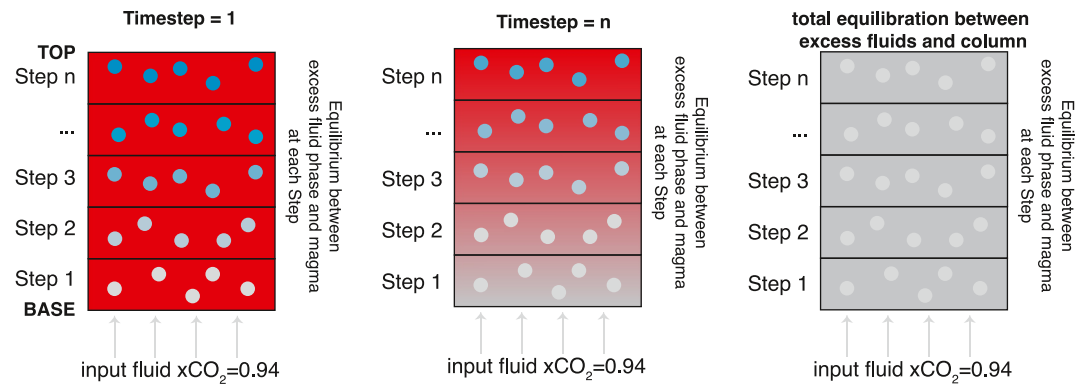
Figure 2. Conceptual representation of the model of interaction between excess fluid phase and magma. We consider a column of magma through which an excess fluid phase wth $xCO_2 = 0.94$ is transported in bubbles of 1 mm diameter. At each step within the column (corresponding to 10 MPa) the excess fluid re-equilibrates with the melt. This leads to a change of both the exsolved and dissolved volatiles, represented as changing color of the column for the different timesteps.

we can consider our initial assumption valid (Figure 3). Stokes timescale were calculated assuming a magma column density of $\rho = 3,000$ kg/m^3 and a gas density of $\rho_G = 1,000$ kg/m^3 (corresponding to pure CO_2 at 400 MPa), which is an underestimate of the density contrast within the entire plumbing system and thus our estimates are conservative and the assumption of equilibrium between excess fluid phase and melt is verified.

At shallower depths ($\sim$100 MPa), bubble growth increases exponentially, and the assumption of thermodynamic equilibrium fails; our results are thus trustable only at higher pressures, in deeper regions of the feeding systems.

The model is purely thermodynamic and it does not account for multiphase flow within the volcano plumbing system. We focus on the average relative motion of the gas phase with respect to the melt + crystal phases,
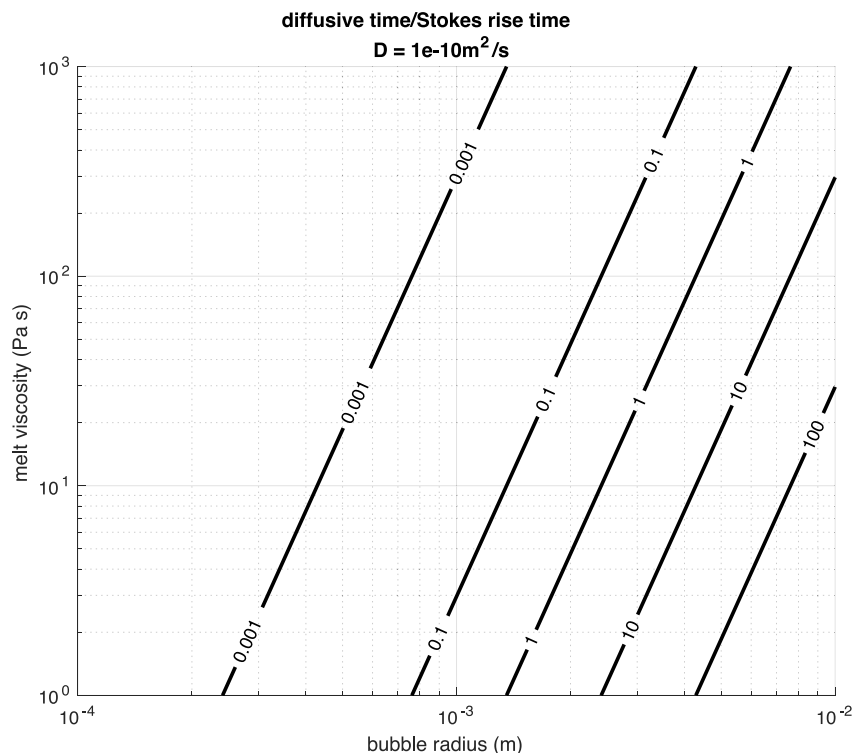

Figure 3. Ratio of diffusive over Stokes time scales for a diffusion coefficient $D = 1 \times 10^{-10}$ m^2/s, appropriate for CO_2. Isolines represent constant ratios, at varying bubble radii and magma viscosity.
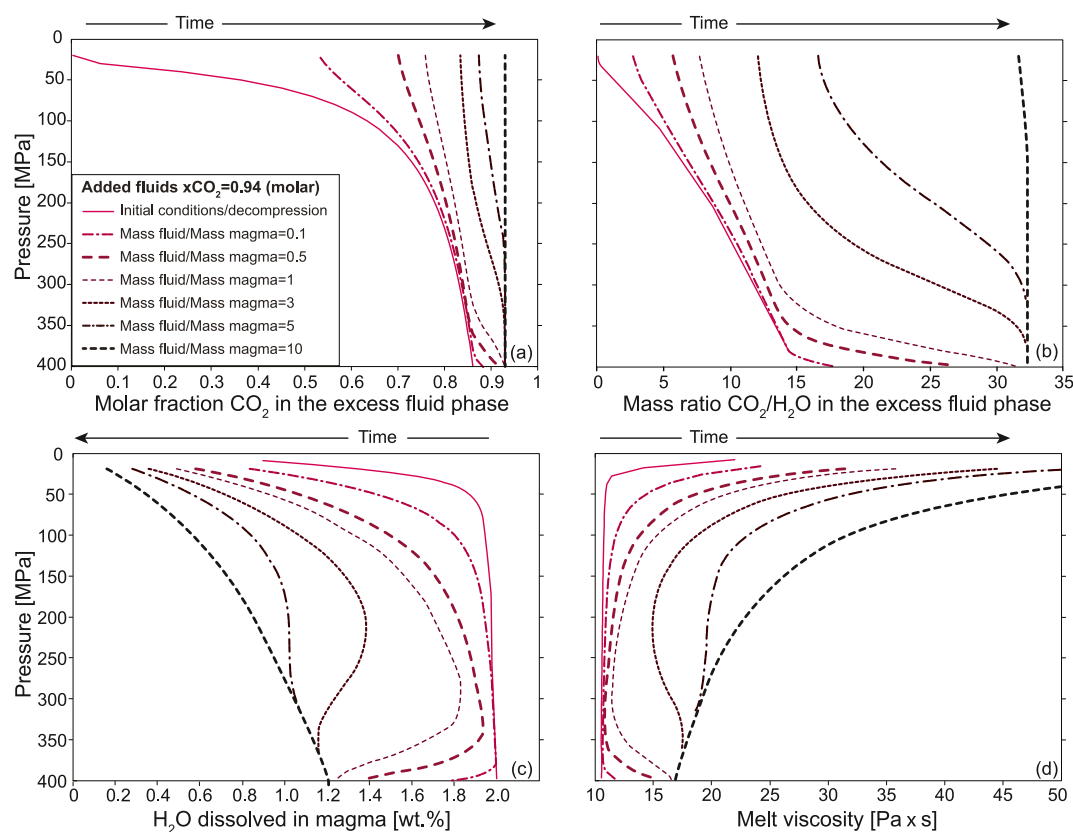
Figure 4. Variation of the chemistry of the excess fluids, dissolved H_2O and melt viscosity at different pressures (i.e., depths) resulting from the interaction between CO_2-rich fluids and magma within the plumbing system. The colors show the fraction in mass of injected fluid with respect to the mass of magma residing within the plumbing system. (a) Molar fraction of CO_2 in the excess fluid phase. (b) CO_2/H_2O mass ratio in the excess fluid. (c) H_2O dissolved in magma. (d) Melt viscosity.

testified by the common observation that emitted gas largely exceeds predictions from erupted products (Aiuppa et al., 2010; Allard, 2010; Burton et al., 2007; Edmonds et al., 2022; Métrich et al., 2010; Shinohara, 2008).

At each computational step, the volume of fluid introduced at the base of the column re-equilibrates with the melt, changes composition, moves to a shallower depth, interacts and equilibrates with the resident melt, changes composition and keeps moving upwards. The calculations are based on the same assumptions as those of the "equilibrium exchange mode" presented by Yoshimura and Nakamura (2011).

Our calculations are performed starting from a typical Stromboli magma column (Métrich et al., 2010) that is at thermodynamic equilibrium with its volatiles and has lost all its excess fluids. This initial condition aims at reproducing the phase following a major explosion/paroxysm, when the whole magma column is re-established by magma rising from deeper regions of the plumbing system. The initial total volatile content is set to 2 wt.% H_2O and 2 wt.% CO_2 (i.e., excess CO_2-rich fluids). Lowering the initial CO_2 content down to 0.5 wt% provides virtually identical results (Montagna, 2023).

We consider the injection of a hundredth of a unit mass of CO_2-rich gas coming from depth at the base of the column (at 400 MPa), and its interaction with a unit mass of magma. We simulate the persistent injection of excess CO_2-rich fluids until a sufficient mass of fluids have been injected and the entire magma column is vapor buffered (Figure 2).

4. Results

Our calculations, in agreement with previous models (Yoshimura & Nakamura, 2011), show that fluid-magma re-equilibration takes place from the bottom toward the top of the magmatic column in a non-linear fashion (Figure 2). The bottom-up re-equilibration of the magma column with the percolating fluids results in the rapid modification of the gas chemistry in the shallow portions of the system (<50 MPa), which we consider as a proxy
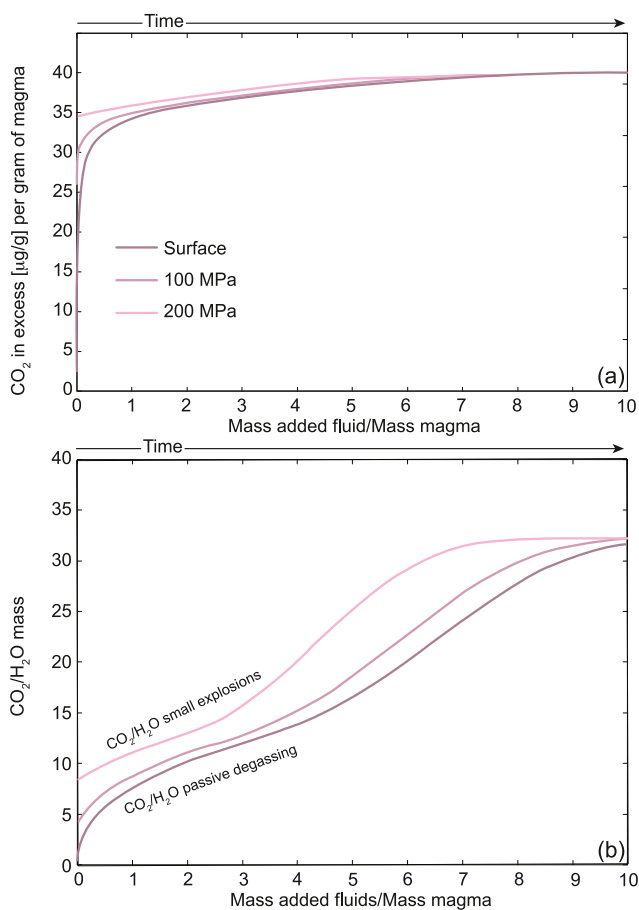
Figure 5. Variation of the chemistry of the excess fluids in equilibrium at different depths as function of the mass ratio of injected fluid and reacted magma. (a) Mass of CO_2 in the excess fluid calculated for 1 g of magma. (b) CO_2/H_2O mass ratio in the excess fluid. The CO_2/H_2O ratio is different between small explosions and passive degassing, because the gas feeding small explosion is sourced from deeper within the plumbing system.

for the surface gas measurements (Figures 4a and 4b). The CO_2/H_2O ratio of the excess fluids decreases toward the top of the magma column for a given ratio of injected fluid and mass of magma within the plumbing system. Flushing the column with an increasing amount of CO_2-rich fluids, leads to the progressive re-equilibration of excess fluids and magma within the plumbing system. Once the mass of excess fluids that has percolated the magma column is roughly 10 times larger than the magma mass, the gases emitted at the top of the column are identical to those injected at the base (i.e., magma and excess fluid are completely re-equilibrated; Figures 4a and 4b). The CO_2 fraction and CO_2/H_2O in the excess fluid phase decrease from the base to the top of the column until all magma is re-equilibrated with the fluid injected at the bottom of the plumbing system (Figures 4a and 4b). This occurs as the CO_2-rich fluids force the release of H_2O from the magma, which dilutes the CO_2 in the excess fluid phase as the front of injected fluids propagates upward.

5. Discussion

We first discuss the results obtained from our simulations and then we apply our findings to the data collected in the period encompassing the 19 July 2020 blast (Figure 1).

The results of our calculations suggest that the progressive re-equilibration of the magma column with the percolating excess fluid is traceable using the continuous measurements of passive degassing and gases emitted during frequent and small strombolian explosions.

Our model predicts that as flushing proceeds, the CO_2 flux of the degassing plume measured at the surface increases rapidly until a mass of excess fluid corresponding to the mass of the magma in the plumbing system has circulated through the column (Figure 5a). Additionally, our calculations show that the CO_2/H_2O ratio of the gases in the degassing plume, which we consider identical to the composition of the excess fluid phase at the top of the magma column (Figure 5b), should be lower than that measured during high frequency and small strombolian explosions that are sourced from deeper within the plumbing system (Figure 5b; Aiuppa et al., 2010).

The interaction between CO_2-rich fluids and the magma column also generates a complex distribution of the dissolved H_2O content in the magma column from the base to the top, which, at decreasing pressure, first increases then decreases in the shallower portions of the column (Figure 4c). This configuration persists until a mass of CO_2-rich fluids equivalent to about three times the mass of magma present within the column, has been flushed (Figure 4d). Because melt viscosity decreases with increasing dissolved H_2O content (Giordano et al., 2008), melt viscosity changes along the column with a pattern that is specular to that of H_2O (Figures 4c and 4d). Specifically, viscosity varies in the range 10–30 Pa s at depth, and it increases rapidly as volatiles exsolve above 100 MPa, reaching up to 70 Pa s. Flushing of CO_2-rich gases leads to magma crystallization (e.g., Caricchi et al., 2018). However, at both 400 and 300 MPa, range over which the viscosity inversion occurs (Figure 4d), the crystal content increases of 14% (Table S1 in Supporting Information S1), which means that even the modest increase of viscosity associated with this amount of crystallization (Caricchi et al., 2007), would not be sufficient to revert the impact of flushing on the distribution of viscosity with depth.

This rheological configuration favors the accumulation of excess fluids at the base of the magma column, without the need of any physical barrier (Jaupart & Vergniolle, 1989; Parfitt, 2004). The accumulation of excess fluids also leads to a gravitationally unstable configuration with lower density (higher fraction of excess fluids) magma underlying denser magma. We suggest that the gravitational destabilization and rapid ascent of this low density, gas-rich magma is ultimately the trigger of large explosions at open conduit volcanoes (Figure 6). We want to stress that while our model provides a mean to trace the potential sequence of events bringing open conduit
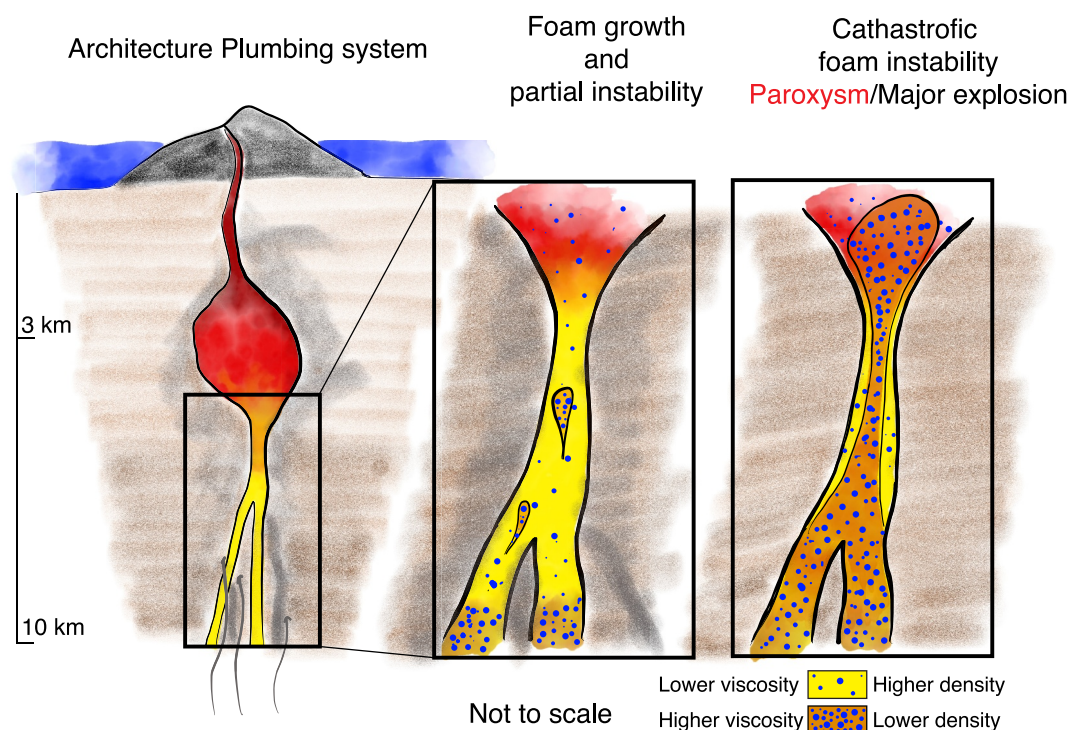
Figure 6. Conceptual model of the triggering mechanism of large/paroxysmal eruptions at Stromboli.

volcanoes toward a critical state, potentially culminating into a large or paroxysmal eruption, many potential and complex feedbacks can act to ultimately avert one of such extreme events.

5.1. Application to Stromboli

We present new data for H_2O and CO_2 collected at Stromboli in a 1-year long interval encompassing the 19 July 2020 blast (Figure 1). Gas plume monitoring is conventionally limited to the more easily detectable CO_2 and sulfur dioxide (Figure 1; Aiuppa et al., 2009, 2010), while in-plume measurement of volcanic water (H_2O), the most abundant volcanic gas species, are challenged by the high and variable atmospheric background (Métrich et al., 2021). From post-processing of a set of gas plume observations taken at Stromboli in a 1-year long interval encompassing the 19 July 2020 blast (Figure 1), we find that the explosion itself is followed by venting of an especially water-rich gas. The CO_2/H_2O (mass) ratios ranges between 0.1 and 0.4 during July 20–31 (the 2020 ratio average is ∼0.9), the H_2O flux is exceptionally high (∼9,400 t/d) on July 22 and remains three times (∼3,300 t/d) above the 2020 yearly average (∼1,050 t/d) during July 20–31. The CO_2/H_2O (mass) ratio oscillates widely before the blast, but the most CO_2-rich composition in our data set is observed on July 6 (CO_2/H_2O of 9.2), 2 weeks before the blast. These measurements provide novel constraints to anchor models for the processes that lead to a paroxysmal explosion.

The data reported in Figure 1 show the 19th of July 2021 explosion was preceded by a progressive increase of CO_2 emission at relatively constant H_2O/CO_2 ratio. We first test if these measurements can be explained by the injection of magma from depth. To test this hypothesis, we performed decompression calculations using SOL-WCAD (Papale et al., 2006) considering the same magma used for the flushing calculations (Metrich et al., 2010) containing 2 wt.% H_2O and 2 wt.% CO_2. The results show that the ascent (i.e., decompression) of a batch of magma results in the decrease of the CO_2 and CO_2/H_2O ratio in the excess volatile phase (Figure 7). This is the opposite of what we measured (Figure 1a) and therefore the ascent of a single batch of magma does not seem responsible for the 19th of July 2020 explosion.

We now use our calculation to show how the flushing of CO_2-rich gas through a column of magma can account for several measurements and observation collected in 2020. For instance, both the increase of CO_2 flux preceding the explosion (Figure 1b) and the distinct compositions measured in the passive degassing plume and during small
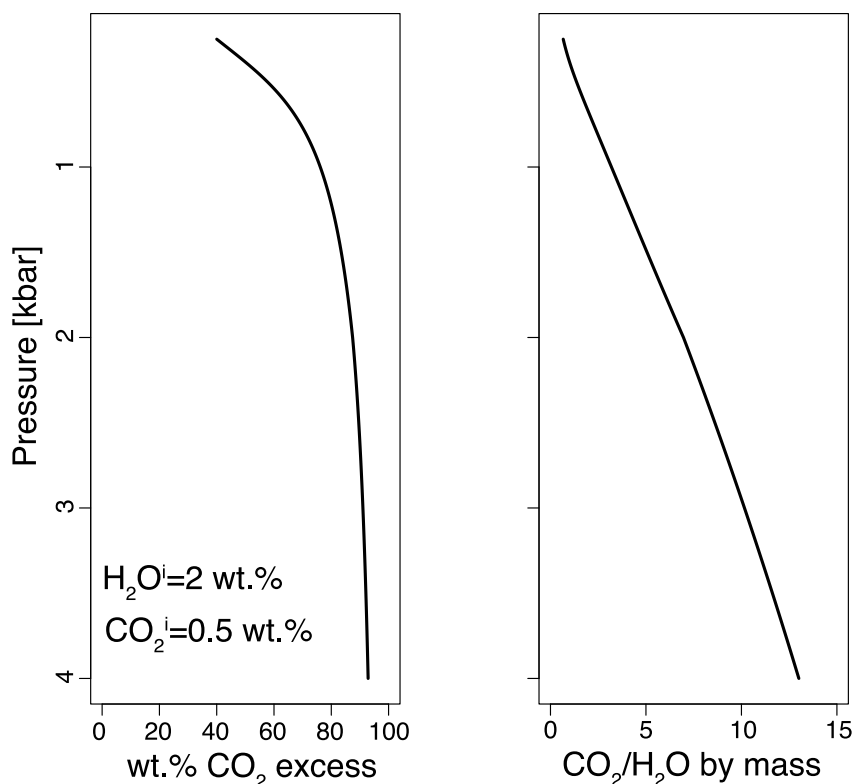
Figure 7. Composition of excess volatile phase for a magma undergoing decompression. (a) Composition of the excess fluid phase (*x* axis) at different depths/pressures (*y* axis) for a mafic magma (see main text; Métrich et al., 2010) with a total volatile content of 2 wt.% H_2O and 2 wt.% CO_2 undergoing decompression at equilibrium. (b) CO_2/H_2O ratio for the excess volatile phase in equilibrium with the compressing magma.

explosions predicted by our model (Figures 4b and 5b) agree with gas monitoring data at Stromboli (Figure 1b; Aiuppa et al., 2010, 2021; Burton et al., 2007). The injection of CO_2-rich magma into the upper portions of the plumbing system has been already proposed as a potential trigger mechanism for the paroxysmal eruptions at Stromboli (Allard, 2010). However, the conceptual model involves the accumulation of excess volatiles at physical discontinuities (Aiuppa et al., 2021; Allard, 2010) and, therefore, requires an ad-hoc physical barrier to drive gas accumulation, for which evidence is difficult to provide. Our calculations show that the increase of magma viscosity at the base of the column caused by the addition of a CO_2-rich excess fluid phase and the consequent release of dissolved H_2O (Giordano et al., 2008; Vona et al., 2011), provides a mechanism for gas accumulation without the need of ad-hoc physical barriers (Figure 4d).

The size of the paroxysms has been already related to the volume of foam ultimately triggering these anomalously explosive events (Aiuppa et al., 2021). The rate of growth of the foam layer is directly related to the rate of fluid input, the mass of magma within the plumbing system and the time since the beginning of the accumulation of excess fluids. Thus, considering the passive degassing flux as comparable to the rate of fluid input at the base of the column, and taking the onset of the increase in the CO_2 concentration measured in the passive degassing plume (together with the increase of the CO_2/H_2O ratio; Figures 1a and 1b) as the onset of excess fluid accumulation, the size of an impending paroxysm can be calculated. To assess the velocity of growth of the foam layer we first consider the CO_2 flux measured at the onset of the increase of CO_2 measured before the 19th of July 2020 event (∼300 t/day; Figure 1b). We first assume that this flux is conserved throughout the magma column, and we convert it into a vertical ascent velocity assuming a cylindrical magma column of constant radius 2.5 m (Harris & Ripepe, 2007; Figure 8b). We obtain a vertical ascent velocity around 5×10^{-4} m/s. The Stokes ascent velocity of bubbles of 1 mm radius (likely an overestimate of the bubble size at 12–15 km depth; Polacci et al., 2009) at the base of the magma column, where the calculated viscosity is around 15 Pa s (Figures 4d and 8b), is lower than 5×10^{-4} m/s. This implies that to conserve the gas flux measured at the surface excess fluid must accumulate at the base of the magma column resulting in the vertical expansion of a foam layer. With these assumption,
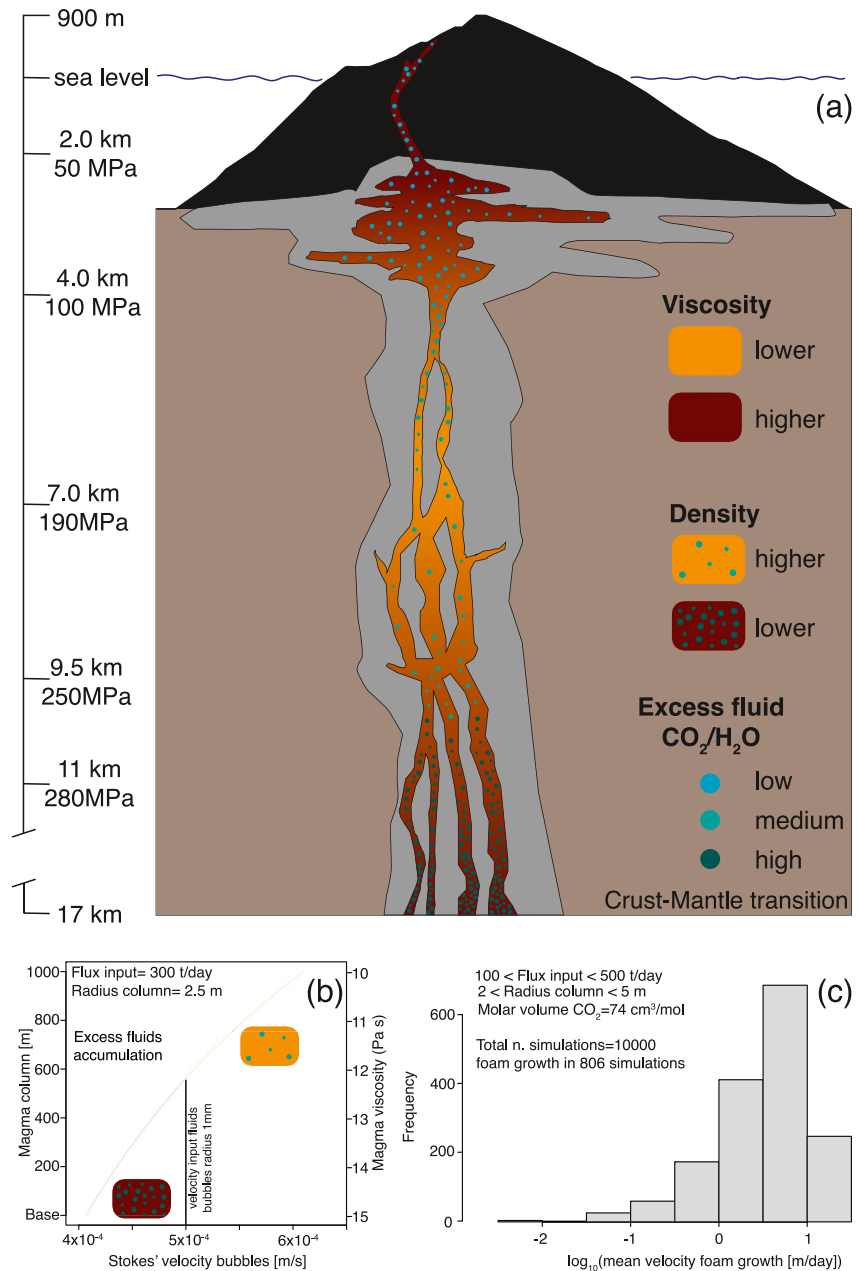
Figure 8. Schematic representation of the plumbing system of Stromboli volcano and results of the calculations of magma foam growth velocity. (a) The schematic figure is redrawn from Aiuppa et al. (2010). The gray region represents completely solidified or highly crystallized magma. The color shading provides an illustration of the variation of magma viscosity while the magma column reaches equilibration with the flushed fluid phase. The color of the bubbles is a function of the CO_2/H_2O ratio of the excess fluid phase. (b) Variation of the stoke ascent velocity of a bubble of 1 mm radius over a magma column length of 1,000 m. The viscosity varies linearly from the base to the top of this portion of the plumbing system and is 15 Pa s at the base and 10 Pa s at the top. The vertical black line shows the velocity of fluid ascent for a daily CO_2 flux of 300 t. (c) Distribution of mean velocity of foam growth calculated from Monte Carlo simulations.

considering the mean velocity of foam growth as the mean difference between the vertical ascent velocity of excess fluid at the base of the column (calculated from the flux measured at the surface) and the Stokes ascent velocity of the bubbles (also at the base of the column), we obtain a vertical foam growth rate of about 4 m/day.

The calculations above depends on several assumptions and parameters that are difficult to estimates. For instance, for a wider conduit or lower input fluxes, no fluids will accumulate at the base of the magma column.
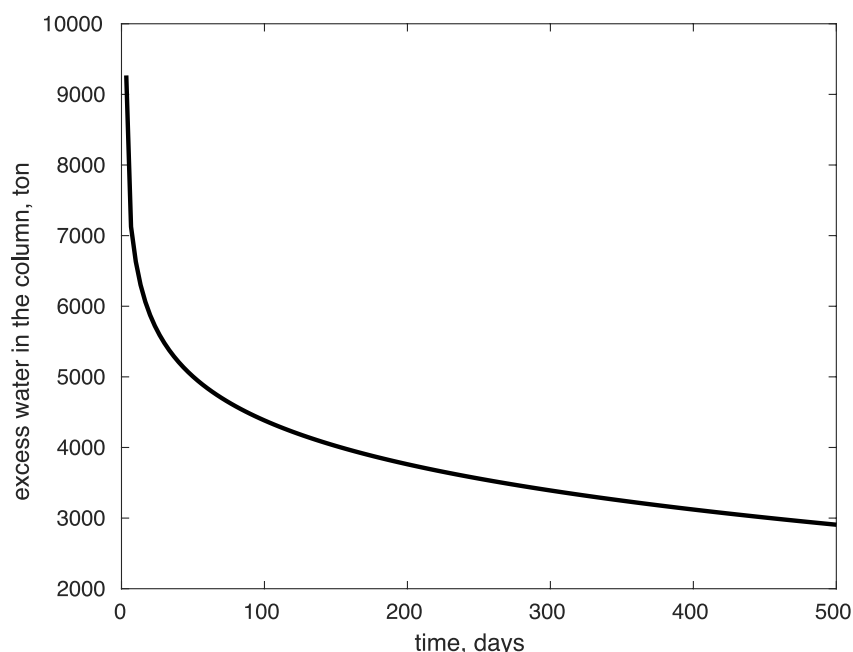
Figure 9. Calculated excess water in the magma column after the refilling due to a major/paroxysmal eruption.

Thus, we performed 10,000 Monte Carlo simulations to estimate the likelihood of excess fluid accumulation. We vary the input fluxes between 100 and 1,000 t/day and the column radii between 2.5 and 5 m. We find that in about 10% of the simulations the conditions lead to growth of a foam layer at the base of the magma column and obtain a distribution of rate of vertical foam growth with a maximum around 1–10 m/day (Figure 8c). The thickness of the foam layer for the 19th of July 2020 paroxysm has been estimated at about 200 m (Aiuppa et al., 2021) and we suggest that the flushing of a CO_2-rich fluid at the base of the plumbing system was responsible for the growth of this foam layer. Considering the most likely rates of foam growth we calculated from our Monte Carlo simulations (Figure 8c) that the time from the onset of flushing to eruption would have been between 20 and 200 days, which is of the same order of magnitude of the time interval between the onset of CO_2 and CO_2/H_2O increase recorded by gas monitoring and the paroxysm of July 2020 (i.e., ∼75 days; Figure 1).

The last important observation that should be accounted for, is the enhanced release of H_2O following the explosion of the 19th of July 2020, which persisted for tens of days, and it is accompanied by a progressive increase of the CO_2/H_2O ratio (Figure 1a). The refilling of the plumbing system by deeply sourced magma can account for the H_2O released immediately after the explosion (Figure 9) but cannot explain its duration nor the progressive increase of CO_2/H_2O. We calculate the amount of excess H_2O present within the magma column once the CO_2 flushing process resumes. The results show that initially the interaction between CO_2-rich fluids and magma results in the release of copious amounts of H_2O initially dissolved in the magma column. For a column of 2.5 m diameter and a flux of 300 t/d CO_2 we obtain values of exsolved H_2O decreasing from 9,000 to 4,000 tons for the first 100 days from the onset of CO_2-magma interaction (Figure 9). These values are comparable to those measured after the 19th of July 2020 paroxysm (Figure 1a). We suggest therefore that the elevated H_2O emissions observed after the 19th of July explosion signaled the refilling of the plumbing system and the renewed interaction between CO_2-rich gases and magma within the plumbing system that eventually led to three larger explosions in November 2020 (Figure 1). Speculatively, it is also possible that portions of the gas-rich magma responsible for the 19th of July explosion were still present within the plumbing system and possible were responsible for the three events in short succession in November 2020.

6. Conclusions

Several studies have proposed that larger explosion at open conduit volcanoes are triggered by the rapid ascent of gas-rich magmas from depth (Aiuppa et al., 2009, 2010, 2021; Edmonds et al., 2022; Métrich, 2005; Métrich et al., 2021; Petrone et al., 2022). However, existing models require that the accumulation of low-density gas-rich

magma at depth is the consequence of the presence of a physical barrier at depth and cannot determine which mechanism is ultimately responsible for the sudden ascent of this gas rich magma toward the surface. This would make the forecasting of these unexpectedly large explosions virtually impossible.

Our calculations of equilibration between a percolating excess fluid phase and magma within a vertically extended plumbing system show that this interaction naturally leads to the progressive growth of a gas-rich foam layer at the base of the magma column, which removes the requirement of an ad-hoc physical barrier at depth. The growth of the gas-rich and low-density foam at depth can be traced providing a unique opportunity to identify the approach to a large or paroxysmal eruption and quantifying its potential magnitude. The destabilization might occur in days as testified by the observed interaction between deeply sourced and gas-rich magmas with magmas stored at shallow depth at Stromboli volcano (Petrone et al., 2022).

We propose a novel model for the triggering of large and paroxysmal eruptions at open conduit volcanoes, which can be traced using continuous gas monitoring data. The possibility of tracing the process of accumulation of gas at depth is extremely important as it could serve to mitigate the hazard associated with frequently erupting open conduit volcanoes.

Data Availability Statement

Software for this research is available in these in-text data citation references: Montagna (2023) [GNU General Public License]. The volcanic gas results illustrated in Figure 1 are reported in Table S2.

References

Aiuppa, A., Bertagnini, A., Métrich, N., Moretti, R., Di Muro, A., Luizzo, M., & Tamburello, G. (2010). A model of degassing for Stromboli volcano. *Earth and Planetary Science Letters*, *295*(1–2), 195–204. https://doi.org/10.1016/j.epsl.2010.03.040

Aiuppa, A., Bitetto, M., Delle Donne, D., La Monica, F. P., Tamburello, G., Coppola, D., et al. (2021). Volcanic CO_2 tracks the incubation period of basaltic paroxysms. *Science Advances*, *7*(38). https://doi.org/10.1126/sciadv.abh0191

Aiuppa, A., Bitetto, M., Francofonte, V., Velasquez, G., Bucarey Parra, C., Giudice, G., et al. (2017). A CO_2 -gas precursor to the March 2015 Villarrica volcano eruption. *Geochemistry, Geophysics, Geosystems*, *18*(6), 2120–2132. https://doi.org/10.1002/2017GC006892

Aiuppa, A., Federico, C., Giudice, G., Giuffrida, G., Guida, R., Gurrieri, S., et al. (2009). The 2007 eruption of Stromboli volcano: Insights from real-time measurement of the volcanic gas plume CO_2/SO_2 ratio. *Journal of Volcanology and Geothermal Research*, *182*(3–4), 221–230. https://doi.org/10.1016/j.jvolgeores.2008.09.013

Allard, P. (2010). A CO_2-rich gas trigger of explosive paroxysms at Stromboli basaltic volcano, Italy. *Journal of Volcanology and Geothermal Research*, *189*(3–4), 363–374. https://doi.org/10.1016/j.jvolgeores.2009.11.018

Andronico, D., Del Bello, E., D'Oriano, C., Landi, P., Pardini, F., Scarlato, P., et al. (2021). Uncovering the eruptive patterns of the 2019 double paroxysm eruption crisis of Stromboli volcano. *Nature Communications*, *12*(1), 4213. https://doi.org/10.1038/s41467-021-24420-1

Blundy, J., Cashman, K. V., Rust, A., & Witham, F. (2010). A case for CO_2-rich arc magmas. *Earth and Planetary Science Letters*, *290*(3–4), 289–301. https://doi.org/10.1016/j.epsl.2009.12.013

Burton, M., Allard, P., Muré, F., & La Spina, A. (2007). Magmatic gas composition reveals the source depth of slug-driven Strombolian explosive activity. *Science*, *317*(5835), 227–230. https://doi.org/10.1126/science.1141900

Caricchi, L., Burlini, L., Ulmer, P., Gerya, T., Vassalli, M., & Papale, P. (2007). Non-Newtonian rheology of crystal-bearing magmas and implications for magma ascent dynamics. *Earth and Planetary Science Letters*, *264*(3–4), 402–419. https://doi.org/10.1016/j.epsl.2007.09.032

Caricchi, L., Sheldrake, T. E., & Blundy, J. (2018). Modulation of magmatic processes by CO_2 flushing. *Earth and Planetary Science Letters*, *491*, 160–171. https://doi.org/10.1016/j.epsl.2018.03.042

Corsaro, R. A., & Miraglia, L. (2022). Near real-time petrologic monitoring on volcanic glass to infer magmatic processes during the February–April 2021 paroxysms of the South-East Crater, Etna. *Frontiers in Earth Science*, *10*. https://doi.org/10.3389/feart.2022.828026

Delle Donne, D., Lo Coco, E., Bitetto, M., La Monica, F. P., Lacanna, G., Lages, J., et al. (2022). Spatio-temporal changes in degassing behavior at Stromboli volcano derived from two co-exposed SO_2 camera stations. *Frontiers in Earth Science*, *10*, 972071. https://doi.org/10.3389/feart.2022.972071

Edmonds, M., Liu, E., & Cashman, K. (2022). Open-vent volcanoes fuelled by depth-integrated magma degassing. *Bulletin of Volcanology*, *84*(3), 28. https://doi.org/10.1007/s00445-021-01522-8

Giordano, D., Russell, J. K., & Dingwell, D. B. (2008). Viscosity of magmatic liquids: A model. *Earth and Planetary Science Letters*, *271*(1–4), 123–134. https://doi.org/10.1016/j.epsl.2008.03.038

Girona, T., Costa, F., & Schubert, G. (2015). Degassing during quiescence as a trigger of magma ascent and volcanic eruptions. *Scientific Reports*, *5*, 1–7. https://doi.org/10.1038/srep18212

Harris, A., & Ripepe, M. (2007). Synergy of multiple geophysical approaches to unravel explosive eruption conduit and source dynamics—A case study from Stromboli. *Chemie der Erde*, *67*, 1–35. https://doi.org/10.1016/j.chemer.2007.01.003

Iacovino, K., Matthews, S., Wieser, P. E., Moore, G. M., & Bégué, F. (2021). VESIcal Part I: An open-source thermodynamic model engine for mixed volatile (H_2O-CO_2) solubility in silicate melts. *Earth and Space Science*, *8*(11), 1–55. https://doi.org/10.1029/2020ea001584

Jaupart, C., & Vergniolle, S. (1989). The generation and collapse of a foam layer at the roof of a basaltic magma chamber. *Journal of Fluid Mechanics*, *203*, 347–380. https://doi.org/10.1017/S0022112089001497

Laiolo, M., Delle Donne, D., Coppola, D., Bitetto, M., Cigolini, C., Della Schiava, M., et al. (2022). Shallow magma dynamics at open-vent volcanoes tracked by coupled thermal and SO_2 observations. *Earth and Planetary Science Letters*, *594*, 117726. https://doi.org/10.1016/j.epsl.2022.117726

Métrich, N., Bertagnini, A., & di Muro, A. (2010). Conditions of magma storage, degassing and ascent at Stromboli: New insights into the volcano plumbing system with inferences on the eruptive dynamics. *Journal of Petrology*, *51*(3), 603–626. https://doi.org/10.1093/petrology/egp083

Métrich, N., Bertagnini, A., Landi, P., Rosi, M., & Belhadj, O. (2005). Triggering mechanism at the origin of paroxysms at Stromboli (Aeolian Archipelago, Italy): The 5 April 2003 eruption. *Geophysical Research Letters*, *32*(10), L10305. https://doi.org/10.1029/2004GL022257

Métrich, N., Bertagnini, A., & Pistolesi, M. (2021). Paroxysms at Stromboli volcano (Italy): Source, genesis and dynamics. *Frontiers in Earth Science*, *9*, 1–17. https://doi.org/10.3389/feart.2021.593339

Montagna, C. P. (2023). cpmontagna/pyFlushing: November 21, 2023 release (version 1.0) [Software]. *Zenodo*. https://doi.org/10.5281/zenodo.10176157

Newman, S., & Lowenstern, J. B. (2002). VOLATILECALC: A silicate melt-H_2O-CO_2 solution model written in visual basic for excel. *Computers & Geosciences*, *28*(5), 597–604. https://doi.org/10.1016/s0098-3004(01)00081-4

Papale, P. (2018). Global time-size distribution of volcanic eruptions on Earth. *Scientific Reports*, *8*, 1–11. https://doi.org/10.1038/s41598-018-25286-y

Papale, P., Moretti, R., & Barbato, D. (2006). The compositional dependence of the saturation surface of H_2O+CO_2 fluids in silicate melts. *Chemical Geology*, *229*(1–3), 78–95. https://doi.org/10.1016/j.chemgeo.2006.01.013

Papale, P., Moretti, R., & Paonita, A. (2022). Thermodynamics of multi-component gas–melt equilibrium in magmas: Theory, models, and applications. *Reviews in Mineralogy and Geochemistry*, *87*(1), 431–556. https://doi.org/10.2138/rmg.2022.87.10

Parfitt, E. A. (2004). A discussion of the mechanisms of explosive basaltic eruptions. *Journal of Volcanology and Geothermal Research*, *134*(1–2), 77–107. https://doi.org/10.1016/j.jvolgeores.2004.01.002

Petrone, C. M., Mollo, S., Gertisser, R., Buret, Y., Scarlato, P., Del Bello, E., et al. (2022). Magma recharge and mush rejuvenation drive paroxysmal activity at Stromboli volcano. *Nature Communications*, *13*(1), 7717. https://doi.org/10.1038/s41467-022-35405-z

Polacci, M., Baker, D. R., Mancini, L., Favretto, S., & Hill, R. J. (2009). Vesiculation in magmas from Stromboli and implications for normal Strombolian activity and paroxysmal explosions in basaltic systems. *Journal of Geophysical Research: Solid Earth*, *114*(B1), B01206. https://doi.org/10.1029/2008JB005672

Rosi, M., Bertagnini, A., & Landi, P. (2000). Onset of the persistent activity at Stromboli volcano (Italy). *Bulletin of Volcanology*, *62*(4–5), 294–300. https://doi.org/10.1007/s004450000098

Shinohara, H. (2008). Excess degassing from volcanoes and its role on eruptive and intrusive activity. *Reviews of Geophysics*, *46*(4), L13309. https://doi.org/10.1029/2007RG000244

Vergniolle, S., & Métrich, N. (2022). An interpretative view of open-vent volcanoes. *Bulletin of Volcanology*, *84*(9), 83. https://doi.org/10.1007/s00445-022-01581-5

Voloschina, M., Métrich, N., Bertagnini, A., Marianelli, P., Aiuppa, A., Ripepe, M., & Pistolesi, M. (2023). Explosive eruptions at Stromboli volcano (Italy): A comprehensive geochemical view on magma sources and intensity range. *Bulletin of Volcanology*, *85*(6), 34. https://doi.org/10.1007/s00445-023-01647-y

Vona, A., Romano, C., Dingwell, D. B., & Giordano, D. (2011). The rheology of crystal-bearing basaltic magmas from Stromboli and Etna. *Geochimica et Cosmochimica Acta*, *75*(11), 3214–3236. https://doi.org/10.1016/j.gca.2011.03.031

Watson, E. (1991). Diffusion of dissolved CO_2 and Cl in hydrous silicic to intermediate magmas. *Geochimica et Cosmochimica Acta*, *55*(7), 1897–1902. https://doi.org/10.1016/0016-7037(91)90031-Y

Yoshimura, S., & Nakamura, M. (2010). Chemically driven growth and resorption of bubbles in a multivolatile magmatic system. *Chemical Geology*, *276*(1–2), 18–28. https://doi.org/10.1016/j.chemgeo.2010.05.010

Yoshimura, S., & Nakamura, M. (2011). Carbon dioxide transport in crustal magmatic systems. *Earth and Planetary Science Letters*, *307*(3–4), 470–478. https://doi.org/10.1016/j.epsl.2011.05.039